

Pattern dynamics in a two-dimensional gas discharge system

Takeshi Sugawara , Kunihiko Kaneko

*Department of Basic Science, Graduate School of Arts and Science,
The University of Tokyo, 3-8-1, Komaba, Meguro, Tokyo 153-8902, Japan*

Abstract Reaction-diffusion equation model for a 2-dimensional gas discharge system is introduced in close relationship with the recent experiment by Nasuno [1]. The model shows formation of spots, molecule-like organization of a cluster of spots, moving of spots, and intermittent collapse and recreation of spots, in agreement with experiments. The pattern dynamics are classified into distributed, localized, and moving spots, and periodic wave pattern. The phase diagram displayed against the current and pressure has some agreement with that observed in the experiment. Dynamic change of spot numbers as well as the structure of the spot cluster is studied in terms of the collective flow of charge, and discussed as chaotic itinerancy.

1 Introduction

Pattern dynamics in nonequilibrium systems have been studied over decades, in fluid, chemical reaction-diffusion systems, liquid crystal, and so forth. The extensive studies in the field have elucidated a rich variety of pattern dynamics, together with the advances in theoretical analysis [2] ~ [11].

One field in the pattern dynamics that is not so well explored in comparison with the above examples, is a discharge system. When a strong voltage is applied between the electrodes, electric discharge appears through the gas filled in the chamber. The discharge often forms a complex spatiotemporal pattern, as has been studied theoretically and experimentally ([12]~[18]).

In such discharge system, due to the conservation of electric charge, there is some constraint among each local discharge process. Viewed as pattern dynamics, this means existence of global coupling among local dynamical processes. On the other hand, global coupling among nonlinear units often shows a non-trivial collective motion, as has been extensively studied as collective motion in globally coupled dynamical systems. Now in the discharge system, there exists interplay between collective motion in globally coupled systems and pattern dynamics by local nonlinear dynamics. As a study of nonlinear system, it is interesting to search for some novel dynamic

state, due to this interplay.

Indeed, there is a beautiful experiment by Nasuno, suggesting such novel, non-trivial dynamics[1]. He set up an experiment consisting of two parallel plates between which electric charge flows. By controlling the voltage and current, he found formation of spots, organization of 'molecular-like' structures of spots, complex motions of them, including the dynamics what he called teleportation.

In the present paper we introduce a phenomenological model on 2-dimensional (2D) gas discharge system, as a coupled electric circuit subjecting a global constraint, to describe the salient features observed in Nasuno's experiment, and to make further predictions. As a theoretical model, we adopt a two-layer model that describes well a glow discharge system [12]~[14]. This two-layer model consists of non-linear resistive part and linear resistive part. By extending this two-layer model, we construct a coupled dynamical system consisting of elementary circuit systems, each of which represents the process at the interior between square electrodes. By taking spatial continuum limit, this model is reduced to a two-dimensional reaction diffusion (RD) system with global constraint. Through extensive simulations of the model, we will show several phases of the pattern dynamics, and reproduce most salient features in Nasuno's experiment.

The outline of the paper is as follows. In Sec.2, the experiment by Nasuno is briefly described. In Sec.3, we present some assumptions in order to reproduce the experiment and then construct a coupled circuit system as a model on the gas discharge experiment. In Sec.4, results of extensive simulations are presented, with classification of distinctive pattern dynamics as in the phase diagram. Formation of spots, and of cluster of spots are numerically observed, as well as the dynamics of creation and annihilation of spots, while the dynamical systems mechanism of the process is discussed, as well as demonstrations of correspondence with the experiment. In Sec.5, summary, discussion and future perspectives are

presented.

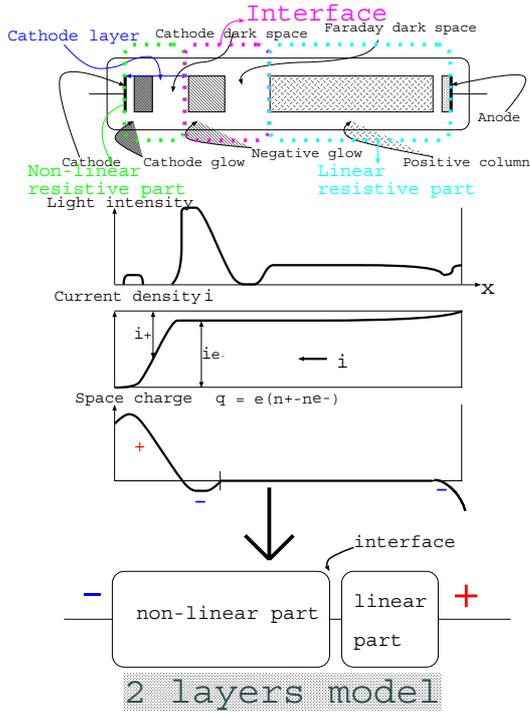


Figure 1: Schematic figure of 2 layers model for glow discharge. We consider that the glow discharge structure consists of two parts, the non-linear resistive region and the linear one.

2 Experiment

Here we briefly describe a remarkable experiment by Nasuno([1]). In the experiment, two square electrodes are immersed in low pressure air P and connected to a dc power source ϵ and a variable resistor R_{ex} . Current I supplied the electrodes by ϵ is kept constant, which is different from the conventional discharge experiments. By controlling I and P , complex pattern dynamics in subnormal glow discharge region was observed. By increasing current I , the pattern dynamics of discharge changes as follows.

- Just after onset of glow discharge, one isolated spot with a typical size (that is, a humped bell-like light intensity distribution) appears. The spot wanders irregularly on the square plane.
- With the increase of I , the number of isolated and wandering spots increases.
- As I is increased further, some spots form a molecule-like localized structure, which is called *cluster*. This cluster also wanders on the plane.

- With the further increase of I , the number of spots in the cluster increases leading to various clusters with a variety of configurations of spots. Switching among the different clusters occurs intermittently.
- At much higher I , the excited domain (the area with high light intensity) forms a string or a closed loop.
- Also, Nasuno reported a remarkable phenomenon which he termed 'Teleportation', where annihilation of a spot and immediate recreation of a spot at a distant place was observed. For example, when 3 spots existed, one of them suddenly was extinguished, and then a new spot immediately appeared at a distant position, located in the neighbor of a remaining spot, so that the 3 spot-state is recovered [1].

The phase diagram in terms of I and P is displayed in the paper [1], where the above behaviors are distributed $I - P$ parameter space.

3 Model

3.1 Assumption

Here we introduce an electric circuit model corresponding to the above experiment. The model is at a macroscopic phenomenological level, where discharge process between 2D electrodes is described as *charge transfer process by a coupled circuit system*. For each element, we adopt the so-called "2 layer model" which consists of non-linear resistive part and linear resistive one, as schematically shown in Fig.1. The model has succeeded in explaining several discharge experiments [12]~[14].

To set up the coupled circuit model, we make the following assumptions:

- The experimental condition in Nasuno's experiment is set just beyond the onset of self-sustained discharge, that is, at the region of subnormal glow discharge.
- We describe the phenomena in terms of current density $i(x, y)$ and space charge density $q(x, y)$ because we focus only on the *charge transfer process* between two electrodes, neglecting the other non-essential effects.
- Following the *experiment condition*, we keep total current that flows into electrodes as *constant*.

- In electrodes (represented by 2 dimensional planes), local voltage-current density characteristic is assumed to be S-shaped (with a logarithmic scale), as will be given later. Indeed, this type of characteristic curve is rather common in discharge [19].
- *Gas pressure effect* between electrodes is taken into account, as is known experimentally. According to [14], this effect is effectively described as diffusion of current density that flows between electrodes. Based on the experimental results, we assume a monotonous relation between gas pressure and the diffusion of current density.
- Total space charge remains *constant in time* between electrodes, where complex dynamics can occur (See 3.3).

3.2 Specific Model

The discharge model which we consider here consists of two square electrodes (area S) and the interior, which are under “External circuit” that consists of the dc power source ϵ and the variable resistor R_{ex} , as shown in Fig.2. The total current I flowing into the electrodes is controlled to be constant, according to the experimental setup [1]. Here, each elementary circuit k is connected with the neighboring ones by linear resistor R and is also contacted with “External circuit”. As shown in Fig.2, this elementary circuit consists of a linear resistor, capacitance, linear coil and a nonlinear resistor given by a specific i - v characteristics. The linear resistor r , the region U and the intermediate region correspond to linear resistive layer, the non-linear resistive layer, and the interface in 2-layer model, respectively. Each part is characterized by a linear resistor r , capacitance C , the constant self-inductance l of the coil, while the voltage drop v_k at the non-linear layer follows the i - v characteristics given by a log-scaled S-shaped function of i_k . The total current I is distributed to each element with a current J_k , while its current at B and U is given by j_k and i_k respectively, as shown in Fig.2.

Now, we describe the main discharge system by N ordinary differential equations first, given by N coupled circuits, as shown in Fig 2, and then will consider the spatial continuum limit later. In the model it is assumed that there are some charge flow into the interface (i.e. at “B” in the figure) from the non-linear resistive layer, as will be discussed again in Sec.3.4. Let us represent this flow of *charge density* by s_k . This flow comes from a charge distributed at the interface

between the layers, due to the excitation, ionization and recombination of gas molecules. Since the total space charge Q should be constant in time between electrodes, there is a global constraint on $\sum_k s_k$ as will be discussed again in Sec.3.3.

Now, we derive the equations on the current densities and the charge densities, based on the above setup. Considering the law of the conservation of charge (the first Kirchoff’s rule) at the point A, we get

$$J_k - j_k + \left[-\frac{1}{RC}\{(q_k + s_k) - (q_{k-1} + s_{k-1}) + (q_k + s_k) - (q_{k+1} + s_{k+1})\}\right] = 0, \quad (1)$$

while the law of the conservation of charge at the point B gives

$$j_k - (i_k + \frac{dq_k}{dt}) = \frac{ds_k}{dt}. \quad (2)$$

At the region U, the voltage balance (the second Kirchoff’s rule) leads to the following equation

$$l \frac{di_k}{dt} + v_k - \frac{q_k}{C} = 0. \quad (3)$$

In addition to (1)~(3), we need to consider the above constraint on the constant total charge and constant total current.

$$Q' = \sum_{k=1}^N (q_k + s_k) = const. \quad (4)$$

$$I = \sum_{k=1}^N J_k = const. \quad (5)$$

The charge should be determined as a function of $(\{i_m, q_m\})$, $(m = 1, 2, \dots, N)$ in general. Accordingly we must define s_k satisfying (1)~(5). When the boundary condition is Neumann or periodic, $\sum_{k=1}^N i_k = I = const.$ is satisfied (See appendix). Hence, as $q'_k = q_k + s_k$, s_k ’s are determined so as to satisfy

$$\frac{dq'_k}{dt} = \frac{V}{r} - \frac{q'_k}{rC} - i_k + \frac{1}{RC}(q'_{k-1} + q'_{k+1} - 2q'_k) \quad (6)$$

$$\frac{di_k}{dt} = \frac{q'_k}{lC} - \frac{s_k}{lC} - \frac{v_k}{l} \quad (7)$$

$$I = \sum_{k=1}^N i_k = const. \quad Q' = \sum_{k=1}^N q'_k = const.$$

While each of s_k is generally a function of $(\{i_m, q_m\})$, $(m = 1, 2, \dots, N)$ as above, they should be defined under the constraint

$$\sum_{k=1}^N \frac{di_k}{dt} = 0.$$

Hence s_k satisfies

$$s_k \equiv \frac{i_k}{I} (Q' - C \sum_{k=1}^N v_k).$$

Now, we obtain the following 2-component RD equation, with $D_{q'} = \frac{1}{rC}$, $Q' = \int q' dS$, as (See appendix for details.)

$$\frac{dq'}{dt} = \frac{V}{r} - \frac{q'}{rC} - i + D_{q'} \Delta q' \quad (8a)$$

$$\frac{di}{dt} = \frac{q'}{lC} - \frac{s}{lC} - \frac{v(i)}{l} + D_i \Delta i \quad (8b)$$

$$s \equiv \frac{i}{I} \{Q' - C \int v(i) dS\} \quad (8c)$$

The RD equation (8a)~(8c) is normalized as

$$\tau \frac{dq}{dt} = V - q - ai + \Delta q \quad (9a)$$

$$\frac{di}{dt} = \frac{1}{a} \{q - s - v(i)\} + D \Delta i \quad (9b)$$

$$s \equiv \frac{i}{I} \{Q - \int v(i) dS\} \quad (9c)$$

using dimensionless variables

$$\tilde{i} = \frac{i}{i_c}, \tilde{v} = \frac{v}{v_c}, \tilde{q} = \frac{q'}{Cv_c}, \tilde{t} = \frac{t}{\tau} \quad \text{and redefining}$$

$$\tilde{i} \rightarrow i, \tilde{v} \rightarrow v, \tilde{q} \rightarrow q, \tilde{t} \rightarrow t, \quad \text{respectively,}$$

$$\text{but } \tau = \frac{rC}{I}, a = r \frac{i_c}{v_c}, D' = \frac{D_i}{D_q}, D = \frac{D'}{\tau},$$

$$\xi^2 = rCD_q \text{ (characteristic length).}$$

3.3 Constraint for the constant total charge

Here we discuss the meaning of the constraint of the conservation of the total current. Under the condition of a constant total current I , it is only through charge transfer within the *inside* of the electrodes that spatial charge density distribution at local site changes. Spatial charge distribution at each local site is changed only by generation and extinction of charge due to ionization and recombination, and charge transfer due to the diffusion. The molecular ionization process occurs to change the local charge density given by the change of s_k , while the total charge Q is kept constant in time. Accordingly the total charge Q is constant and remains the initial value Q_0 , which implies that sum of $q_k + s_k$ is constant as the initial sum $\sum_k q_k^0$, i.e. $\sum_{k=1}^N (q_k + s_k) = \sum_k q_k^0$.

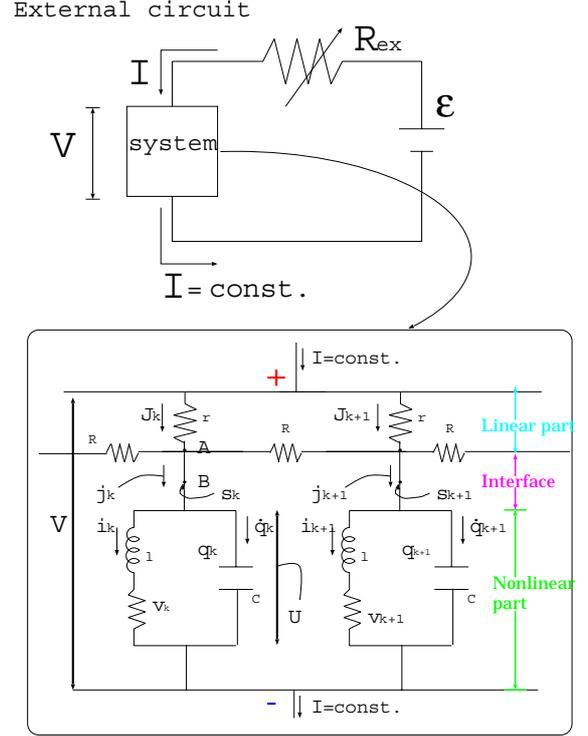


Figure 2: Schematic figure of our 2-dimensional discharge model. Our model system consists of N coupled circuits. The element k is connected with neighbor ones by linear resistor R and with “External circuit”. Although displayed in a one-dimensional representation, what we actually simulated in the paper is a two-dimensional case.

3.4 Flowing charge density

Here we make some remarks on the flowing charge s_k at the point B in Fig 2. The point B corresponds to the interface of the 2-layer model, that is, the position between the “Negative glow” and Faraday dark space, which exists for the steady glow discharge (Fig 1). In this region, electrons flowing from Cathod layer (non-linear resistive layer) combine with positive ions flowing from “Positive column” (i.e., the linear resistive layer). There, some complex processes occur through diffusion, excitation, ionization, and recombination of molecules. Hence there is a transverse flow of charge, so that there exist flowing charge density s_k at B.

For a homogeneous steady glow discharge, on the other hand, this region has no space charge, because it is in a plasma state at any point on 2 dimensional plane (See Fig 1). Furthermore, s_k at B is zero, as the initial state before the discharge. Hence, if a spatially homogeneous state were stable, the flow term s_k would not be necessary. However, as will be shown, for almost all the parameter regions, such homogeneous state is unstable, where charge density q is distributed inhomogeneously in the non-linear resistive layer. In this case, flowing charge density s is also distributed in the interface. Hence we need to consider this term.

After taking a spatial continuum limit, the total flowing charge is given by the spatial integration,

$$h \equiv \int s dS (= Q - \int v(i) dS), \quad (10)$$

where h means the total charge flowing from the non-linear resistive layer into the interface, which is a macroscopic dynamical variable characterizing the global charge transfer process between the non-linear layer and the interface and develops in the direction of the gap. On the one hand, it is pattern dynamics on quasi-two dimensional plane that we observe, which evolves through the reaction-diffusion process between local sites.

3.5 Parameter setting

Hereafter we study the behaviors of the present model given by the equations (9a)~(9c), by controlling the parameters I and D , which are the total current into the system, and a parameter for the gas pressure effect, respectively. Hence the control parameters I and D exactly correspond to those in the experiment, i.e., the total current and the pressure P , respectively. As initial conditions of $i(x, y)$ and $q(x, y)$, we mostly

choose “uniform state i_u, q_u ” with small fluctuations $\eta(x, y)$. Accordingly total current $I (= i_u S)$, total charge $Q (= \int q dS)$ and voltage $V (= V(Q, I))$ are determined initially.

Unless otherwise mentioned, the other parameters are fixed as

$$\begin{aligned} \tau &= 20, \xi^2 = 0.004 \text{ (characteristic length),} \\ a &= 400 \frac{i_c}{v_c}, \text{ and } S = \frac{1}{\xi^2}. \end{aligned}$$

Numerical simulations are carried out by the mesh size 128×128 . Unless otherwise mentioned, we choose a periodic boundary condition.

These parameters are chosen so that a single element satisfies the behavior for a simple discharge (without spatial pattern). Before describing the pattern dynamics of the model, we first show how a single element behaves. Fig 3 is the nullcline of the single element dynamics. The parameter $a (= r \frac{i_c}{v_c})$ is chosen so that the steady state (i_u, q_u) is destabilized when $i_u > i_c$, and thus the single element shows limit cycle oscillation.

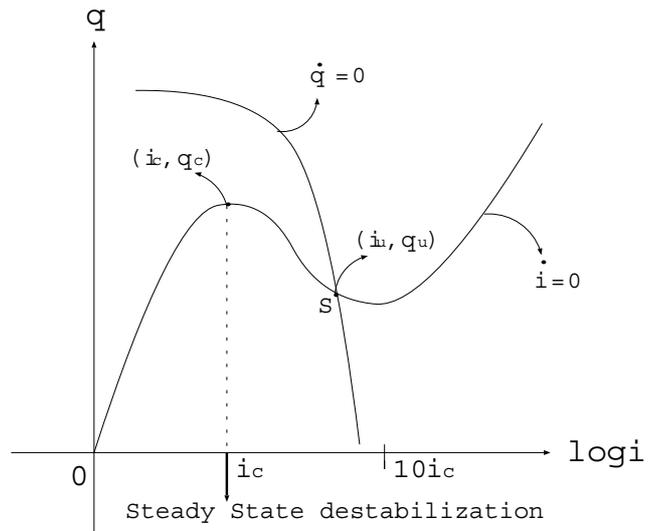


Figure 3: Nullcline of the single element dynamics. Parameter $a (= r \frac{i_c}{v_c})$ is chosen so that the steady state (i_u, q_u) is destabilized when $i_u > i_c$, and the element shows limit cycle oscillation.

4 Phenomena

4.1 Preparation: behavior of each element under the global constraint

In this section, we describe a variety of static and dynamic behaviors in the model (9a)~(9c), which are rich and agree with experimental results.

Before discussing the pattern dynamics in detail, we briefly comment on the behaviors of the system by taking into account only the global constraint, but without spatial diffusion terms (9a)~(9c). In this case, spatial configuration of each element is discarded, but the conservation gives a global coupling. Hence the system is reduced to a globally coupled equation of N limit cycle oscillators given by

$$\tau \frac{dq_k}{dt} = V - q_k - ai_k \quad (11a)$$

$$\frac{di_k}{dt} = \frac{1}{a} \{q_k - s_k - v(i_k)\} \quad (11b)$$

$$s_k \equiv \frac{i_k}{I} \left\{ Q - \sum_{m=1}^N v(i_m) \right\} \quad (11c)$$

$$\left(\tau = \frac{rC}{r}, \quad a = r \frac{i_c}{v_c}, \quad V = a \frac{I}{N} + \frac{Q}{N} \right)$$

Such system with global coupling among limit cycle oscillators has been studied over a decade. For example, some interesting behaviors such as clustering, nontrivial collective motion and chaotic itinerancy have been found in a globally coupled map (GCM)[20]. In particular, in the nontrivial collective motion, a macroscopic variable shows an ordered motion, whereas each element dynamics shows chaotic motion[21]~[27]. Indeed, the above model also shows such behaviors that are observed in such globally coupled dynamical systems, with the change of the coupling strength. As for the collective motion, the sum of flowing charge s_k , $\sum_{m=1}^N s_m (\equiv h)$ corresponds to the mean-field for GCM. As an example of collective motion, we have computed the timeseries of h . This oscillation has a period of hundreds or thousands times large of the time scale for each element.

4.2 Global phase diagram

According to our interpretation of the present model (9a)~(9c), the discharge occurs at local site if $i(x, y) \geq i_u$ under $i_u \geq i_c$. Hence we show the pattern dynamics by displaying only the pixels that satisfy $i(x, y) > i_u$, an active region with discharge, by gray.

Here we study the pattern dynamics by changing $i_u (= \frac{I}{S})$ and D , by focusing on the parameter region with $i_u > i_c$, where the discharge phenomena occur. As a 2-dimensional phase diagram with regard to i_u and D , the pattern dynamics we have observed is classified into five phases, as displayed in Fig.4. We first give a brief description of each phase, and will discuss the characteristics of each phase in detail later.

For small $i_u (\sim 1.0)$, there are three phases, depending on the value of D , that are "distributed spot phase (DS)", "localized spots phase (LS)", and moving spot phase (MS), respectively, as shown in Fig 4. In these phases, spots are formed. Discharge occurs locally, only within these spots. Indeed, when $i(x, y)$ is plotted in space, it shows a stepwise increase at the border of each spot, and shows a high plateau within each spot. The pattern dynamics here will be discussed from the configuration of spot patterns and their motion, with which the three phases are classified. For all these three phases, the number of spots increases with i_u in general. For a larger value of i_u , there appears a periodic pattern in space, which we call Periodic Wave (PW) phase. For a further large value of i_u , there is a uniform glow (UG), without spatial inhomogeneity. The behavior of each phase is summarized as follows;

- DS phase — Spots are arranged with some distance on the average, which decreases with the increase of i_u . For small i_u , a few spots are isolated with some distance, while hexagonal pattern of spots appears as i_u is increased. After transient time, these spots are fixed, and do not move.
- LS phase — Spots form several clusters similar to molecular structures, as reported in the experiment by Nasuno. The clusters can show a dynamic, complex behavior with the formation, collapse, and regeneration.
- MS phase — A spot can move by itself in the space, which shows a soliton-like behavior without collapse.
- PW phase — There appears a periodic wave pattern in space and time.
- UG phase — There is a uniform glow, without spatial inhomogeneity.

Collective variable - $\int sdS (\equiv h)$ - As a global measure characterizing the pattern dynamics, the integration of s , $h \equiv \int sdS$ is often useful. In the subsequent subsections, the pattern dynamics will be characterized by the motion of h , which is a collective variable. Now we discuss the pattern dynamics, by referring to the change of this collective variable h .

4.3 DS phase

Isolated steady spots Starting with initial condition $i(x, y) = i_u + \eta(x, y)$, competition for

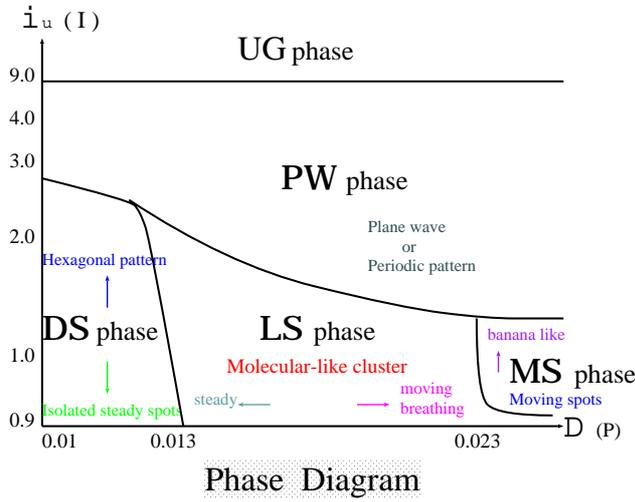


Figure 4: Phase diagram as function of $i_u (= \frac{I}{S})$ and D . Vertical axis is log-scaled. Global property of the model is roughly classified into five phases under $i_u > i_c$.

current among elements occurs, resulting in instability of the homogeneous state. This leads to the formation of spots with localized high current. These spots are of the same size. Initially, each spot moves very slowly, and is arranged so that each is located with an equal distance, until a regular, stationary spots pattern is formed.

Hexagonal pattern As i_u is increased, the number of spots is increased. As the number is increased with the increase of i_u , the distance between spots is decreased. As i_u becomes larger from 1.5 to 2.0, a regular hexagonal pattern of spots is formed, as shown in Fig.5. The formation of this regular lattice of spots is understood as a weak repulsion between neighboring spots.

Behaviors at the boundary between DS and other phases As i_u is increased toward the boundary to the PW phase, the spots start to breathe, and their size (and shape) change, while the distance between spots still remains almost equal as in Fig 6(a-1). The collective variable h changes intermittently, too, corresponding to the pattern dynamics (Fig 6(a-2)).

Around the boundary between the DS and LS phases, the characteristic wavelength disappears, and the configuration of spots become irregular, while spots start to show a bursting behavior, as well as splitting, as in (Fig 6(b-1)). The change of h is also irregular, as well as that of pattern dynamics(Fig 6(b-2)).

In the experiment by Nasuno, the behavior corresponding to this phase is not observed. We

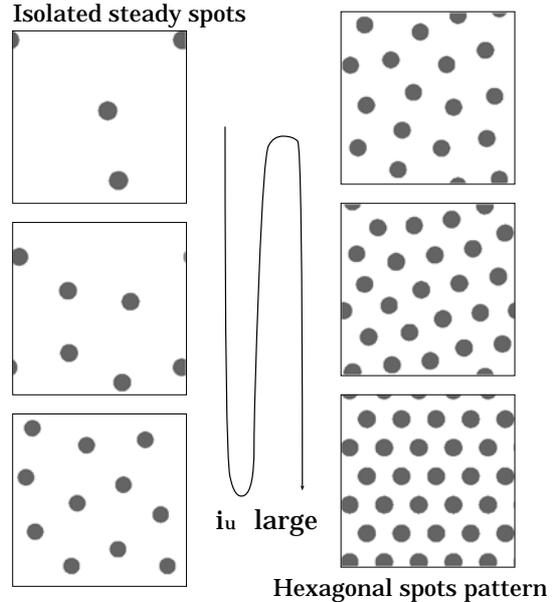


Figure 5: Steady patterns observed in the DS phase. Spots are of the same size under fixed D . Initially, each spot moves very slowly, and is arranged so that it is located with the equal distance. As i_u is increased, the number of spots is increased. As the number is increased with the increase of i_u , the distance between spots is decreased. Left—Isolated steady spots. $i_u = 0.87, 0.93, 1.0$ in the order from the top to bottom with, $D=0.01$. Right—Hexagonal spots pattern. $i_u = 1.2, 1.5, 2.0$ in the order from the top to bottom with $D=0.01$. The mesh size here is 256×256

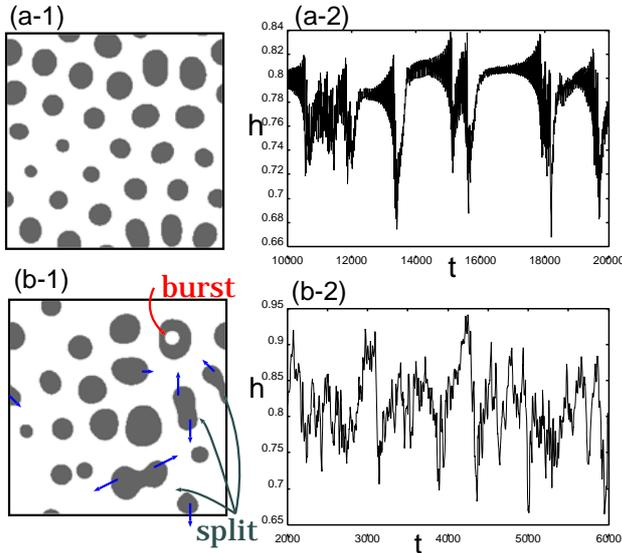


Figure 6: Behaviors at the boundary between the DS and PW phases(a) and at the boundary between the DS and LS phases (b). The left figures (1) give snapshots of pattern dynamics, while the time series of the integration of flowing charge $h(= \int s dS)$ corresponding to them are plotted in (2)(right). In (a), the spots start to breathe, and the size changes, while the distance still remains almost equal. In (b), the characteristic distance is distributed, leading to an irregular pattern. (a) $i_u = 2.4, D = 0.01$, (b) $i_u = 2.0, D = 0.012$, mesh size 256×256

expect that the range of the change of pressure in the experiment is not sufficient to detect this phase, and expect that it is observed by making gas pressure P much lower.

4.4 LS phase

For small $i_u (\sim i_c)$, one spot appears at first, and as i_u is increased, the number of spots increases, through successive split of the original spot. Spots are not completely stable in time, and some of them collapse after breathing. As replication and extinction of spots are repeated, a cluster of spots is formed. For small i_u , the number of spots changes between 1 and 2, while the range of the number of spots that the system can take increases with i_u . Some of the generation processes are displayed in Fig 9.

Phase diagram within the LS phase By measuring the dependence of the maximal number of spots on i_u and D , the phase diagram within the LS phase is depicted as shown in Fig. 7, where the maximal number of spots is given in the $D - i_u$ parameter space. When k spots

exist at maximum, for example, we write *the case* “ M_k ” hereafter. On the other hand, if n spots exist at a moment, we call *the state* “ sp_n ”. Indeed, the configuration of the phases in the phase diagram of Fig.7 obtained from our model agree rather well with that obtained experimentally with regard to the current and pressure[1].

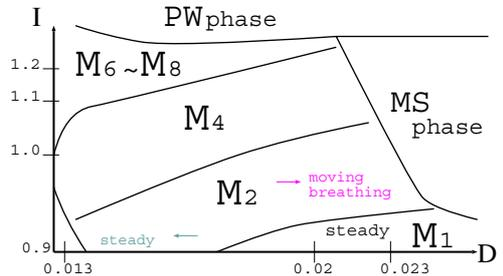


Figure 7: Phase diagram of the LS phase. The behaviors in the LS phase are classified in terms of the maximal number of spots, and plotted as a phase diagram in the $D - i_u$ parameter space. Note that, in this phase diagram, “ M_n ” shows the case in which the maximal number of spots is n .

Localized cluster of spots; molecule-like structure

In the following, we discuss dynamics of a localized cluster of spots. After spots are generated by splitting, they separate up to some distance. Thus they form a chain-like structure, a localized structure like a molecule. As the distance between spots is increased and a spot is separated from a cluster very slowly, it starts breathing. Following the amplification of this oscillation, the spot collapses. After this collapse, split of some other spot(s) follows, and the number of spots returns to the maximal under the given value of i_u . In this way, a cluster of spots is sustained.

When the maximal number of spots ≥ 6 , there appears a variety of configurations for the cluster, as shown in Fig 8, as examples for complicated clusters. Depending on which spot splits to which direction, there appears a different form. Over a long time span, one can observe a variety of forms of clusters .

In a long time scale, a cluster wanders slowly on a 2-dimensional space, since the configuration after reconstruction of a cluster is slightly different from the original, even if they are similar. After the split of a spot, there remains some asymmetry between the two spots, which causes a wandering motion of a cluster. We show two examples of such wandering cluster, by displaying successive snapshot patterns in Fig. 10, where

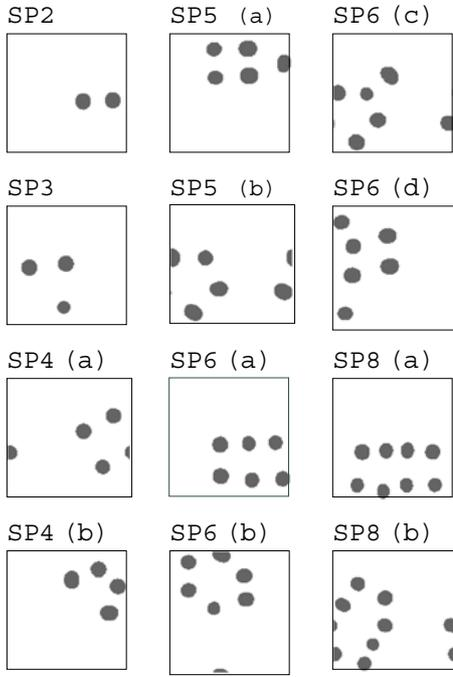


Figure 8: Snapshots of typical clusters, $sp_2 \sim sp_8, D=0.014, sp_2, i_u=0.93, sp_3, i_u=0.934, sp_4(a), i_u=0.98, sp_4(b), i_u=1.01, sp_5(a), i_u=1.1, sp_5(b), i_u=1.06, sp_6(a), i_u=1.1, sp_6(b), i_u=1.1, sp_6(c), i_u=1.1, sp_6(d), i_u=1.1, sp_8(a), i_u=1.15, sp_8(b), i_u=1.15$

the maximum number of spots is 2 (M_2) for Fig 10(a) and 4 (M_4) for Fig, 10 (b), respectively. The motion of cluster is not unidirectional, but its direction changes irregularly. This irregular motion arises since the two spots when splitted are not completely identical. (See also the next subsection for the interpretation by the dynamics of h).

Dynamics of the collective variable h corresponding to the change in the spot number

When the number of spots changes, the transfer of charge is altered drastically. Hence, it is relevant to study the number change in relationship with the collective variable h , i.e., the integration of the flowing charge. In Fig 11(a),(b), (c), we show the time series h for M_2, M_3 and M_4 cases. We plot the time series of h (in (a-1),(b-1),(c-1)), as well as the orbit in the phase space, by embedding the time series of h into three dimensional phase space with the use of $h(t), h(t+1), h(t+2)$.

For all the cases, h increases with the spot number n . When the spot number stays at some value, h remains almost constant. Note that h value is mainly determined by the spot number of the moment sp_n , and is almost independent of the maximal number M_k for a given condition. For example, h for sp_2 under M_2 is almost

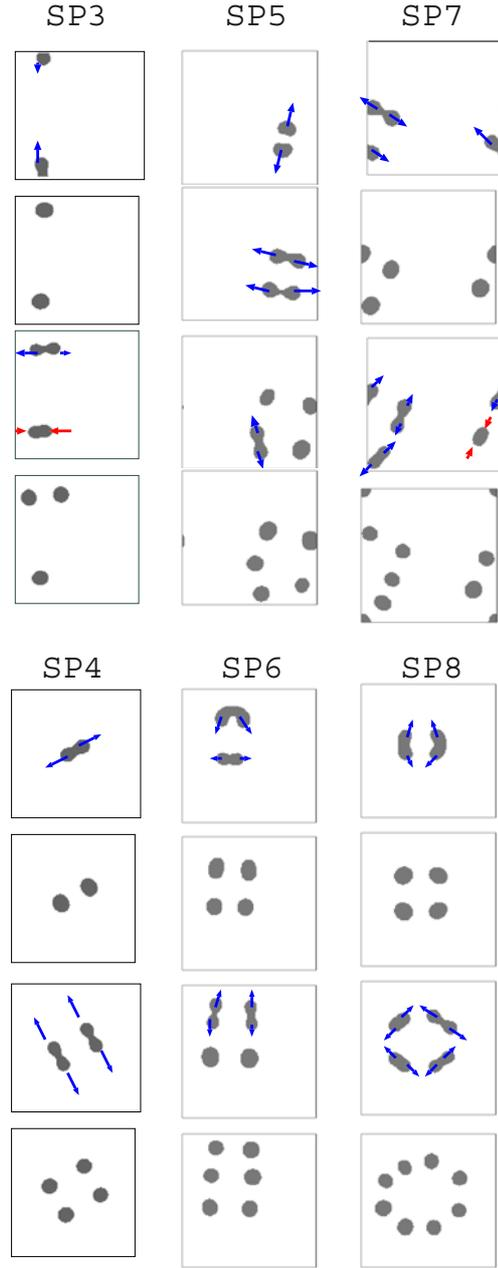


Figure 9: Generation processes of $sp_3 \sim sp_8$. sp_3 : $sp_1 \rightarrow sp_2 \Rightarrow sp_2 \rightarrow sp_3 \Rightarrow sp_3$ cluster ($i_u=0.939, D=0.014$). sp_4 : $sp_1 \rightarrow sp_2 \Rightarrow sp_2 \rightarrow sp_4 \Rightarrow sp_4$ cluster ($i_u=0.98, D=0.014$). sp_5 : $sp_2 \rightarrow sp_4 \Rightarrow sp_4 \rightarrow sp_5 \Rightarrow sp_5$ cluster ($i_u=1.06, D=0.013$). sp_6 : $sp_2 \rightarrow sp_4 \Rightarrow sp_4 \rightarrow sp_6 \Rightarrow sp_6$ cluster ($i_u=1.08, D=0.013$). sp_7 : $sp_2 \rightarrow sp_4 \Rightarrow sp_4 \rightarrow sp_7 \Rightarrow sp_7$ cluster ($i_u=1.1, D=0.013$). sp_8 : $sp_2 \rightarrow sp_4 \Rightarrow sp_4 \rightarrow sp_8 \Rightarrow sp_8$ cluster ($i_u=1.1, D=0.013$).

identical with that of sp_2 under M_4 . When the system stays at a state with given sp_n ($n \leq N$), it is clearly seen as each plateau in the time series of h , or a region with residence of an orbit around a fixed point in the phase space. With the breathing of spots, h also starts to oscillate, and in the phase space picture, the orbit spirals out of a fixed point, leading to a switch to a state with a different number of spots.

Consider the case M3 or M4. There the decrease of the number of spots occurs as $(sp_4 \rightarrow sp_3 \rightarrow sp_2 \rightarrow sp_1)$, successively. During this decrease, the system stays at each state with an intermediate spot number, for some time interval, while the return process $sp_1 \rightarrow sp_2 \rightarrow sp_3$ (or sp_4), is relatively rapid, without staying long at each intermediate state. (The state sp_1 is unstable, and the orbit exits immediately). These decrease and increase in the spot number are repeated. We also note that the switching process observed here is true for a state with a higher number of spots, as have been numerically confirmed up to sp_8 .

In the three-dimensional representation of the phase space from the time series of h , it seems to be possible to assign an each state of a given spot number with a saddle, that has one-dimensional stable manifold, and two-dimensional unstable manifold, with an unstable focus. The attraction and repulsion of each orbit around a saddle is seen whenever the orbit passes through a given sp_n state. Each state of a given spot number is approached from a certain direction, and the orbit spirals out from it. This process is analogous to that observed in Shilnikov chaos. In the Shilnikov chaos, however, the spiral motion is stable, giving a stable 2-dimensional manifold for a focus, while a third direction gives an unstable manifold. In contrast, in the present case, the former is unstable, and the third direction gives a stable manifold. It is expected that the instability here leads to irregular wandering of spots. However, we should note that when h increases monotonously before the orbit passes over sp_n with maximal n , the dynamics follows a behavior like the saddle-node bifurcation (as can be seen in Fig. 11). The nature of the saddle point is different between when the system approaches sp_n and when it leaves.

As the phenomena occur in a high-dimensional dynamical system, however, this description by low-dimensional dynamical systems may be insufficient, and description as chaotic itinerancy may be more appropriate[20, 21], although the detailed analysis is left for the future.

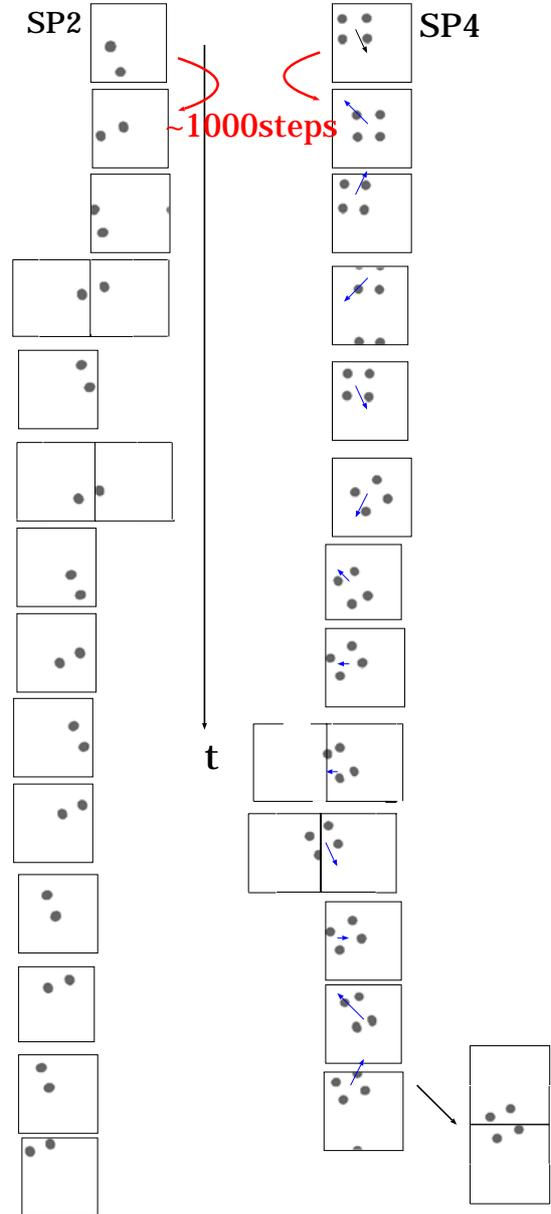


Figure 10: A sequence of snapshots for sp_2, sp_4 state. We see that the positions of sp_2, sp_4 shift in time due to the asymmetry for splitting. In a long time scale, the clusters appear to be wandering. $sp_2:i_u = 0.93$, $sp_4:i_u = 0.98$, $D = 0.014$

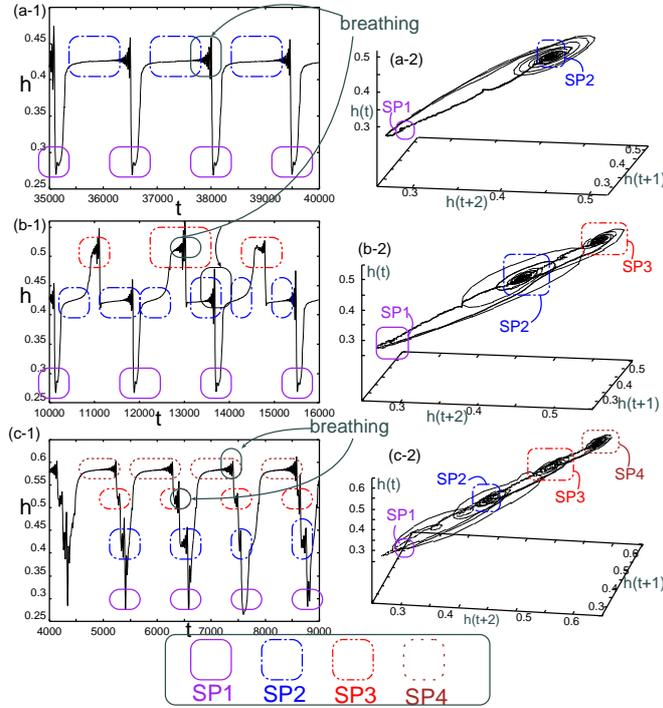


Figure 11: (a) The case M_2 ($i_u=0.93$), (b) The case M_3 ($i_u=0.939$), (c) The case M_4 ($i_u=0.98$), (1) Time series of h , (2) The embedded orbit of h into 3 dimensional phase space. h has a sole value corresponding to each state $sp_1 \sim sp_4$ with respect to different i_u under fixed D . $D = 0.014$

Transition rules between several clusters
Here we study transition-rules between clusters in some detail.

As the increase of the spot number occurs through the splitting of a spot, there exists a certain transition rule from a state with a lower number of spots to that with a higher number. Here we display the paths of generating sp_n ($n = 2, \dots, 8$) through the splitting process (see Fig.12). As shown, each cluster with the larger number of spots is systematically generated from a *specific* state with a smaller number. Note that there are several states with different configuration of spots for a given number of them, when it is larger than or equal to 6.¹

This transition rule of clusters is enriched with the increase of i_u . In Fig.13, the change of rule is plotted, corresponding to the pattern in Fig 12, where the solid upward and broken downward arrows show multiplication of spots by splitting and their collapse by breathing, respectively, while the thickness of the arrows shows the frequency of such processes observed. The change of transition rules is summarized as follows.

¹Here we display only the states generated by splitting, while complicated process involving collapse of spots is not included.

- When i_u is small, only the transition $sp_1 \rightleftharpoons sp_2$ occurs.
- As i_u is increased, the states sp_3 and $sp_4^{(1)}$ (which is one type of the 4-spot state) appear, with the transitions $sp_1 \sim sp_3$, $sp_1 \sim sp_4^{(1)}$.
- With the further increase of i_u , another 4-spot cluster with asymmetric configuration appears, denoted by $sp_4^{(2)}$. Now there are transitions $sp_1 \sim sp_3$, $sp_1 \sim sp_4^{(1)}$, $sp_1 \sim sp_4^{(2)}$.
- As i_u is increased further, the states $sp_5 \sim sp_8$ appear, with a variety of transitions. These transitions are divided into two groups as in Fig.12, that is those among $sp_1 \sim sp_4^{(1)}$ and among $sp_1 \sim sp_4^{(2)}$.

Note that with the increase of the spot number, both the configurations and transitions are diversified.

- When the maximum number of spots is larger than or equal to 4, there exist clusters with the same number but different configurations. Those states give almost the same value of h , and they are degenerated in the representation of h .
- When the maximum number of spots is larger than or equal to 6, the collapse process is diversified, and indeed is more diverse than that displayed in Fig 13.
- The transitions between the degenerate states, i.e., different configuration states with the same number of spots, cannot occur directly. Only after the increase or decrease of the spot number, they can mutually change, as in Fig. 13.

Correspondence with the experiment

The pattern dynamics we observed here agree rather well with that observed experimentally [1] as is summarized as follows.

- The global phase diagram on the spot number with regards to i_u and D (pressure) agree rather well.
- The cluster of spots forms a molecule-like structure, whose structures are identical. These structures are similar to that observed on the experiment. (In the experiment, the molecular state is so far reported up to the spot number 6 mainly). In our

case, the number of spots shows intermittent decrease, while by comparing the state that is dominant in time, the agreement is clear.

- When the maximal spot number is larger than or equal to 6, a variety of forms of clusters appears, both in our model and in experiment.
- An interpretation of teleportation in the term of Nasuno: Nasuno reported phenomena in which one of the two spots disappears, and right after it, a new spot appears around the remaining spot. Since it is observed as if one of the spots moved to a distant place within a very short time scale, he called this phenomenon as 'teleportation'. According to our results, we can give a possible interpretation to this phenomenon. In the M_2 regime, one of the spots disappears intermittently as we have mentioned. Following this disappearance of one spot, the remaining spot divides into two. Note that the time interval between the disappearance of one spot and the division of the remaining spot is very short. Then, within the resolution of experimental measurement, this process is observed as if one spot teleported to the location close to another spot.

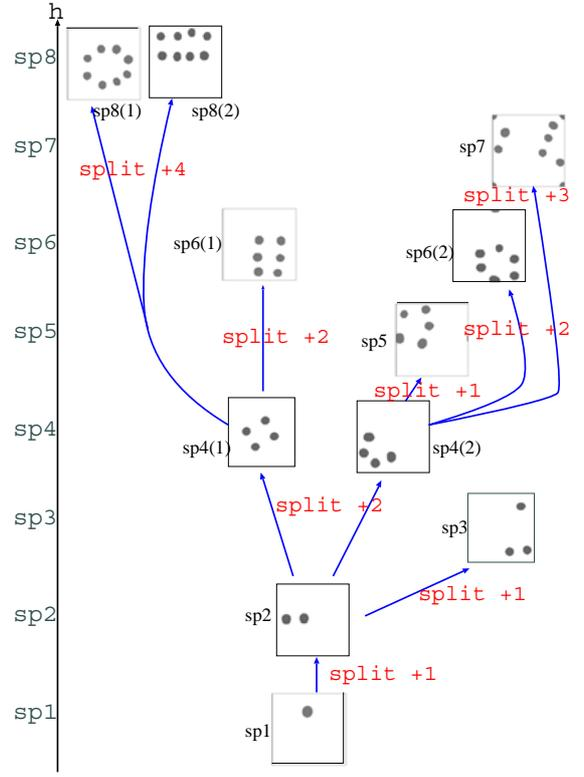


Figure 12: Paths to create state with a higher number of spots, sp_n ($n=2, \dots, 8$) by splitting. Note that only the states generated by splitting are displayed, and some other complicated ones, which are generated as a result of extinction of spots by breathing, are not displayed here.

4.5 Moving spot phase

At this phase a single spot moves in the space. For $0.93 \leq i_u \leq 1.0$ in Fig 4, a single *moving spot* appears, while multiple moving spots are observed with the increase of i_u .

Soliton-like spot Here a single spot (abbreviated by “ ms_1 ”) moves without split or collapse. The locus of a spot is displayed in Fig 14, with a periodic boundary condition, where a solid line shows the center of mass of ms_1 . The center of mass is defined by the mean position among sites with $i(x, y) \geq i_u$. Of course, if the spot is completely symmetric in shape, it cannot move. The motion of a spot is due to asymmetry in the shape of ms_1 , and indeed the spot is deviated from a circle slightly.

The nature of motion changes with the increase of i_u . For small i_u value, that is just above the onset of the appearance of ms_1 , the motion is linear with a constant speed. (See Fig 14, $i_u = 0.925$). With the increase of i_u , the motion starts to have a curvature, and the locus is bended. This curvature is increased with

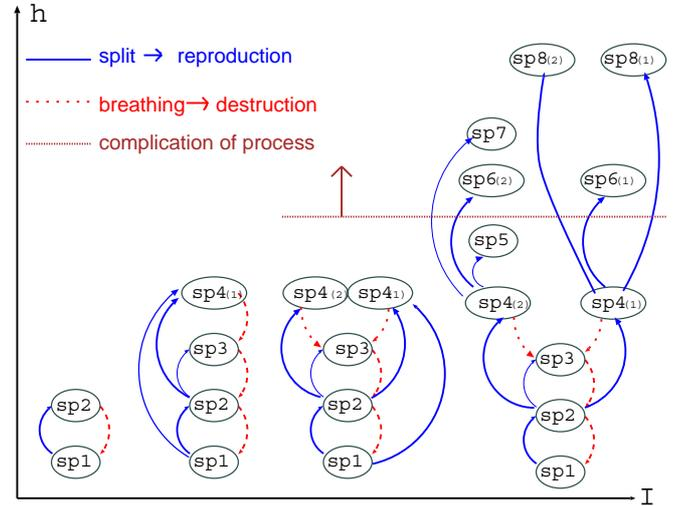


Figure 13: Schematic figure for transitions among quasi-stationary states. The solid upward and broken downward arrows show multiplication processes of spots by splitting and extinction process of them by breathing, respectively. The thickness of the arrows indicates the frequency of the processes. The typical cluster configurations in the present figure are shown in Fig 12.

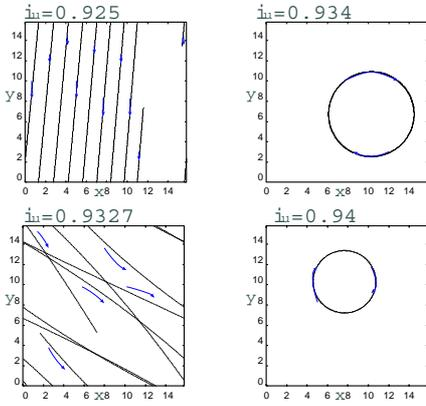


Figure 14: Dependence of the orbits of a single moving spot on the value of i_u , under periodic boundary condition. We show the direction of movement of ms_1 with an arrow. $D = 0.027$, mesh size 256×256 .

i_u , and the locus shows a circle, as in Fig 14, $i_u = 0.934, 0.94$. With the increase of curvature, the speed also increases.

For this motion of spot, the choice of boundary condition may be more crucial. For example, to compare with an experiment, the periodic boundary condition may not be relevant. Hence, we have also made some simulations with Neumann boundary condition, as shown in Fig 15. With reflection at the boundary, the motion becomes more complex, depending on the ratio of the radius of curvature of the orbit to the electrode size $S^{\frac{1}{2}}$.

Multiple moving spots As i_u is increased further, a single moving spot splits, leading to moving multiple spots (Fig 16). Here, the moving spot is first distorted to extend its tail as spiral. When the tail is small, the spot rotates with it, while as it is larger, the spot is divided into two, which move to the opposite direction (*generation of ms_2*). After the motion of these two spots, collapse of one spot occurs as in the LS phase, and the system comes back to a single spot state. These processes are repeated to lead to a complex motion of spots.

As shown in Fig.16, the spot shape starts to be distorted. This distortion is much clearer, as i_u is further increased, where the system approaches the boundary with the PW phase. There the spot size is larger, and forms a distorted "banana-like" shape. This "banana-like" spot goes straight without collapse.

Periodic wave phase In general, as i_u is increased, each element tends to synchronize with each other, since the effective (attractive) cou-

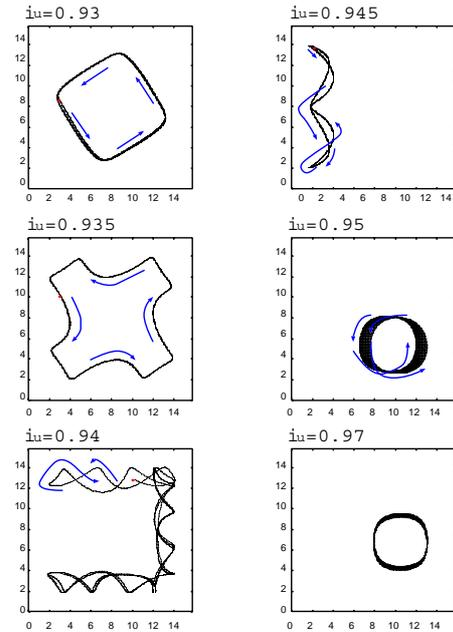


Figure 15: The loci of a single moving spot under the Neumann boundary condition. Arrows show the time course of the spot center. Because the spot reflects at the boundary, the motion is complex as shown for $i_u = 0.94$. On the other hand, it often shows periodic orbits as given for the loci for $i_u = 0.93, 0.935, 0.945$. For $i_u = 0.95, 0.97$, it shows almost circular motion, but the center of the circular orbits shifts gradually. These behaviors depend on the ratio of the radius of curvature of the spot locus to the electrode size $S^{\frac{1}{2}}$. $D = 0.027$

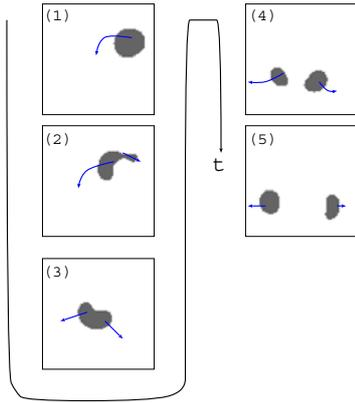


Figure 16: Successive snapshots of multiple moving spots. (1) A single moving spot just before splitting. Here the size starts to expand. (2) It splits into two spots, but one of them is too small and vanishes. The other distorted spot survives and soon begins splitting again. (3) Just before splitting of the distorted spot. (4) Just after splitting of the distorted spot, leading to the state ms_2 . Each spot is separated from each other in the opposite direction. (5) The state ms_2 is maintained, but one of them starts breathing and will vanish before long. $i_u = 1.05$, $D = 0.03$

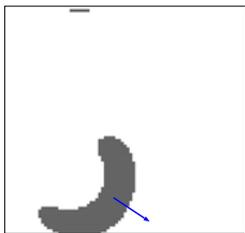


Figure 17: Banana-like spot. A spot is spreaded in the direction perpendicular to the direction of its motion, and finally the banana-like shape is formed. The banana-like spot moves straight without collapse. $i_u = 1.2$, $D = 0.03$

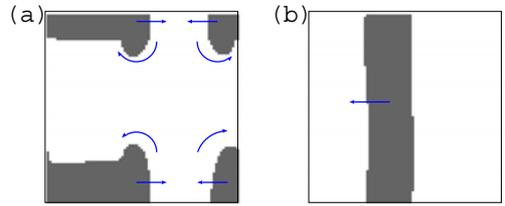


Figure 18: (a) Periodic pattern. The parameter values are $i_u = 5.0$, $D = 0.015$, while the similar patterns appears over a wider parameter range of parameters. (b) Plane wave. $i_u = 5.0$, $D = 0.03$. This plane wave moves in one direction as shown by the arrow.

pling among oscillator elements is stronger. Accordingly, in this regime of a large current, spots no longer exist, and they are replaced by a pattern periodic both in space and time (Fig 18(a)).

Travelling wave One typical pattern observed here is plane wave (Fig 18(b)). As shown, an extended string of discharged region propagates with a constant speed here. A string of concentrated electric discharge is formed over the plate, and it travels with a constant speed.

Stripe pattern Here we briefly describe pattern observed at a different set of parameter values of τ and ξ than that adopted so far. For some parameter values of τ and ξ , we have found a steady pattern, which is different from the DS phase. As an example, we discuss briefly the pattern observed for $\tau = 35$ and $\xi = 0.008$. As i_u is increased, the connected spots form a string and form a stripe pattern as shown in Fig 19. The length of string is increased with i_u , and finally a stripe pattern covers the whole space as in Fig.19. Through the time evolution, a steady pattern is formed, without temporal change. Such pattern formation is also common to that observed in Benard convection with a large aspect ratio.

5 Summary and Discussion

5.1 Summary

To sum up we have introduced a coupled circuit model (9a) \sim (9c), corresponding to a discharge experiment by Nasuno. Mathematically, the model belongs to a class of reaction-diffusion system with global coupling due to the global constraint on the conservation of charge and current. When the total current is large, the system

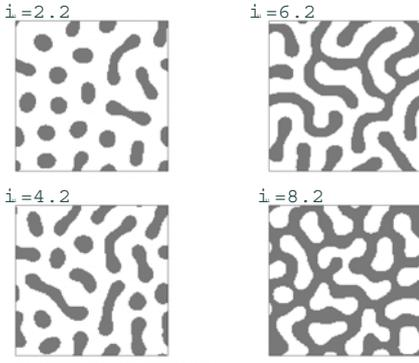


Figure 19: Stripe patten. Spots are extended and connected to form a *string*. As $i_u \nearrow$, many strings are formed, and as a result they are connected with the neighboring strings as shown. Plotted for $i_u = 6.2, 8.2$ (*stripe*).

shows a homogeneous glow, while this homogeneous state is destabilized with the decrease of the current, and a variety of pattern dynamics of discharge is observed, as are classified into four phases, depending on the value of total current and the diffusion constant that corresponds to the pressure value in the discharge experiment.

For the regime with a lower current, the regions with concentrated discharge form spots. They are classified as

- **Distributed Spot phase:** Spots are arranged with some distance, to form a regular array of spots. The phase appears for small D .
- **Localized Spot phase:** A few number of local spots exist, which form a cluster. With the increase of the current the spot number increases. In the cluster spots are arranged like a molecule, while there are several configurations of spots when their number is larger than or equal to 4. Also, we have observed intermittent collapse of spots to decrease their number, and immediate recovery by the splitting of spots. These processes are repeated as a cycle, and with this cycle, the cluster of spots wanders throughout the space.
- **Moving Spot phase:**

For a larger value of D , a shape of a spot is asymmetric, and each spot starts to move by itself. With the increase of the total current the motion changes from linear to circular, while complex motion is observed when the boundary condition is not a periodic one.

Besides these spot phases, we have observed another phase at a high current region:

- **Periodic Wave phase,** where a string of discharged region propagates in space.

These pattern dynamics are characterized by introducing the collective variable $h = \int sdS$, the integration of the flowing charge s_k , which expresses the global charge transfer between the non-linear resistive region and the interface in the direction of the gap. Indeed, h turns out to characterize the number of spots, and the birth-and-death dynamics of spots are represented by the temporal change of h .

5.2 Compariosn with the experiment by Nasuno

The behaviors observed in the LS phase reproduce the phenomena observed in experiments. They include:

- Increase of spot number with the current.
- Molecule-like structures of spots and their variety in shapes.
- Disappearance and recreation of spots, as is termed 'Teleportation' by Nasuno.
- Wandering motion of spots.

loop In the experiment, at a high current region, a loop structure that moves in space is observed. Although a connected string observed in the PW phase is similar to the loops observed in the experiment, one difference here is that in our case the strings are connected through the whole space. Since we have chosen the periodic boundary condition, the edges of the traveling string in Fig 18 are connected, to form a loop, but such travelling string observed is extended to the whole space in our model.

So far, we are not yet confident if the strings in the PW phase correspond to the loops in the experiment. As the loops are not small in contrast to localized spot structures, the influence of the boundary may be important. A suitable choice of boundary condition should be necessary. Instead of periodic or Neumann boundary condition, the Dirichlet boudary may be more relevant to make more accurate correspondence with the experiment. This problem is left for the future.

5.3 Discussion

Novel phenomena in reaction-diffusion system

Since our model belongs to a class of reaction-diffusion system, many of the pattern dynamics observed here are common with those studied therein; formation of spots, array of spots, and strings. Still, the molecule structure of spot cluster, cyclic process of collapse and split of spots, wandering motion of spots are rather novel and characteristic to the present model. For these phenomena, inclusion of global coupling into local reaction-diffusion equations is essential. Systems both with local and global couplings have also been studied in surface catalytic reactions [28, 29], coupled maps[30], and so forth. Search for a novel class of pattern dynamics by global coupling will be interesting in the future.

Collective motion A system with global coupling often shows non-trivial collective motion of a macroscopic variable, such as the mean field of all elements[21]~[27]. Indeed, in the present problem, the macroscopic variable, the integration of charge h , shows a nontrivial collective motion. Characterization of the collective motion will be an important problem for the future. Experimentally, it will be interesting to find relationship between the integration of flowing charge and pattern dynamics.

Itinerancy over clusters with different configurations of spots

Through split and collapse of spots, their number changes, and also transitions between quasi-stationary states with different clusters occur. This transition among quasi-stationary states is found to be governed by a specific rule with regard to the increase or decrease of the spot number. With the aid of the phase-space representation by the macroscopic variable h , this process of itinerancy over different quasi-stationary states with different spot configurations is understood as follows:

Each quasi-stationary corresponds to a state with a different configuration or a different number of spots, sp_n . This state is also represented by a ‘‘saddle’’ point in the dynamical systems of the collective coordinates h . There is a stable manifold to this saddle connecting from a state with a different number of spots, while the orbit spirals out of the saddle, corresponding to the breathing motion of a spot. Although this low-dimensional dynamical description of quasistationary state seems to be rather effective, the transition, indeed, occurs in a high-dimensional dynamical system. Such switching

among effectively low-dimensional states within high-dimensional dynamical system is studied as chaotic itinerancy[20, 21]. The present model gives a novel example of chaotic itinerancy, whose mechanism has to be elucidated in future.

When the number of spots is larger than or equal to 6, a variety of transition processes as well as possible configurations of spots increases drastically. The elucidation of such transition process is left for future as a novel problem in chaotic itinerancy.

Acknowledgement We would like to thank Masaki Sano, Masashii Tachikawa, Akinori Awazu, Koichi Fujimoto, Shin’ichi Sasa, and Teruhisa Komatsu, for discussions and suggestions. The present paper is dedicated to the memory of the late Dr. Satoru Nasuno.

Appendix Derivation of evolution equations

From (1)~(5), we derive 2 component RD equation in terms of current density i , charge density q' (= $q + s$).

(1)~(3) and (5) are respectively

$$J_k - j_k + \left[-\frac{1}{RC}\{(q_k + s_k) - (q_{k-1} + s_{k-1}) + (q_k + s_k) - (q_{k+1} + s_{k+1})\}\right] = 0 \quad (1)$$

$$j_k - (i_k + \frac{dq_k}{dt}) = \frac{ds_k}{dt} \quad (2)$$

$$l \frac{di_k}{dt} + v_k - \frac{q_k}{C} = 0 \quad (3)$$

$$I = \sum_{k=1}^N J_k = \text{const.} \quad (5)$$

From Fig 2, the potential difference between electrodes V is

$$V = \frac{q_k}{C} + \frac{s_k}{C} + r J_k \quad (k = 1, 2, \dots, N) \quad (12)$$

If s_k were independent variables, there would exist $5N$ variables for $4N$ equations. To solve the above equations, we need another constraint for the description of s_k as a function F of $\{i_m, q_m\}$, ($m = 1, 2, \dots, N$)

$$s_k = F(\{i_m, q_m\}) \quad (m = 1, 2, \dots, N)$$

Here, we introduce the coupled circuit model, for which charge flows into the interface region of the 2 layers model under the condition that total charge is kept constant. Accordingly we will

define s_k satisfying constant total charge condition,

$$Q' = \sum_{k=1}^N q'_k = \sum_{k=1}^N (q_k + s_k) = \text{const.} \quad (4)$$

At first, we eliminate J_k, j_k with (1),(2),(12) and modify them to evolutionary equation in terms of q_k, i_k .

By transformation of valuables $q'_k = q_k + s_k$, (1),(2) are respectively

$$j_k = J_k + \frac{1}{RC}(q'_{k-1} + q'_{k+1} - 2q'_k)$$

$$j_k = i_k + \frac{dq'_k}{dt}$$

Accordingly,

$$\frac{dq'_k}{dt} = J_k - i_k + \frac{1}{RC}(q'_{k-1} + q'_{k+1} - 2q'_k) \quad (13)$$

From (12),

$$J_k = \frac{V}{r} - \frac{q'_k}{rC} \quad (14)$$

From (13),(14)

$$\frac{dq'_k}{dt} = \frac{V}{r} - \frac{q'_k}{rC} - i_k + \frac{1}{RC}(q'_{k-1} + q'_{k+1} - 2q'_k) \quad (15)$$

$$\frac{di_k}{dt} = \frac{q'_k}{lC} - \frac{s_k}{lC} - \frac{v_k}{l} \quad (16)$$

Now, from (5),(12) and (4),

$$V = rJ_k + \frac{q'_k}{C} \Rightarrow NV = r \sum_{k=1}^N J_k + \frac{1}{C} \sum_{k=1}^N q'_k$$

$$= rI + \frac{Q'}{C}$$

$$\Rightarrow V = r \frac{I}{N} + \frac{1}{C} \frac{Q'}{N} = \text{const.}$$

Note that $V = \text{const.}$ results from the requirement for $I = \text{const.}, Q' = \text{const.},$ and

$$I = \sum_{k=1}^N J_k = \sum_{k=1}^N \left\{ \frac{dq'_k}{dt} + i_k - \frac{1}{RC}(q'_{k-1} + q'_{k+1} - 2q'_k) \right\}$$

$$= \sum_{k=1}^N \left\{ i_k - \frac{1}{RC}(q'_{k-1} + q'_{k+1} - 2q'_k) \right\}.$$

When boundary condition is Neumann or period one, $I = \sum_{k=1}^N i_k = \text{const.}$ is satisfied. Hence, s_k are determined so as to satisfy

$$\frac{dq'_k}{dt} = \frac{V}{r} - \frac{q'_k}{rC} - i_k + \frac{1}{RC}(q'_{k-1} + q'_{k+1} - 2q'_k) \quad (17)$$

$$\frac{di_k}{dt} = \frac{q'_k}{lC} - \frac{s_k}{lC} - \frac{v_k}{l} \quad (18)$$

$$I = \sum_{k=1}^N i_k = \text{const.} \quad Q' = \sum_{k=1}^N q'_k = \text{const.}$$

While each s_k is generally a function of $(\{i_m, q_m\}), (m = 1, 2, \dots, N)$ as above, they should be defined under the constraint that they satisfy

$$\sum_{k=1}^N \frac{di_k}{dt} = 0.$$

Thus s_k is written as

$$s_k \equiv \frac{i_k}{I} (Q' - C \sum_{k=1}^N v_k).$$

As understood easily, with this form of s_k , it vanishes at the initial homogeneous state, and otherwise proportional to i_k .

By defining s_k in this way, our equations are solvable. Considering spatial continuum limit and pressure effect as diffusion of i , the equations are described as

$$\frac{dq'}{dt} = \frac{V}{r} - \frac{q'}{rC} - i + \frac{1}{RC} \Delta q' \quad (19a)$$

$$\frac{di}{dt} = \frac{q'}{lC} - \frac{s}{lC} - \frac{v(i)}{l} + D_i \Delta i \quad (19b)$$

$$s \equiv \frac{i}{I} \{ Q' - C \int v(i) dS \} \quad (19c)$$

References

- [1] S.Nasuno, *Chaos* 13,1010(2003)
- [2] V.S.Zykov, A.S.Mikhailov, S.C.Müller, *Phys.Rev.Lett.* 78,3398(1997)
- [3] S.Grill, V.S.Zykov, S.C.Müller, *Phys.Rev.Lett.* 75,3368(1995)
- [4] G.Nicolis, I.Prigogine, *Self-Organization in Non-Equilibrium Systems* (Wiley, New York, 1977)
- [5] T.Ohta, M.Mimura, R.Kobayashi, *Phys.D* 34,115(1989)
- [6] T.Ohta, *Phys.D* 151,61(2001)
- [7] S.-I.Ei, M.Mimura, M.Nagayama, *Phys.D* 165,176(2002)
- [8] Y.Nishiura, D.Ueyama, *Phys.D* 150,137(2001)
- [9] A.M.Turing, *Philos.Trans.R.Soc.London* B,237,37(1952)
- [10] P.Gray & S.K.Scott, *Chem.Eng.Sci.* 38,29(1983); *ibid.*, 39,1087(1984); *J.Phys.Chem.* 89,22(1985)
- [11] J.E.Pearson, *Science* 261,189(1993)
- [12] K.G.Müller, *Phys.Rev.A* 37,4836(1988)

- [13] C.Radehaus,R.Dohmen,H.Willebrand,F.-
J.Niedernostheide,Phys.Rev.A 42,7426(1990);
C.Radehaus,H.Willebrand,R.Dohmen,F.-
J.Niedernostheide,G.Bengel,H.-
G.Purwins,Phys.Rev.A 45,2546(1992);
J.Berkemeier,T.Dirksmeyer,G.Klempert,H.-
G.Purwins,Z.Phys.B-
Condensed,Matter, 65,255(1986)
- [14] Ch.Radehaus,T.Dirksmeyer,H.Willebrand,H.-
G.Purwins,Phys.Lett.A 125,92(1987)
- [15] Yu.A.Astrov,Yu.A.Logvin,Phys.Rev.Lett.79,2983(1997)
- [16] Yu.A.Astrov,Phys.Rev.E 67,035203(R)(2003)
- [17] Yu.A.Astrov,H.-G.Purwins, Phys.Lett.A
283,349(2001)
- [18] C.H.Thomas,O.S.Duffendark,Phys.Rev.35,72(1930)
- [19] Y.P.Raizer, *Gas Discharge Physics* (Springer, Berlin, 1991)
- [20] K.Kaneko,Phys.D 41,(1990)
- [21] K.Kaneko,I.Tuda,Complex Systems:Chaos and Be-
yond, Springer(2000)
- [22] K.Kaneko,Phys.Rev.Lett.65,1391(1990)
- [23] T.Shibata,K.Kaneko, Phys.D 124,177(1998)
Phys.Rev.Lett.81,4116(1998);T.Shibata,
T.Chawanya,K.Kaneko,Phys.Rev.Lett.82,4424(1999)
- [24] N.Nakagawa,Y.Kuramoto,Prog.Theor.Phys.89,313(1993)
- [25] D.Dominguez,H.A.Cerdeira,Phys.Rev.Lett.71,3359(1993)
- [26] H.Chate,P.Manneville,Prog.Theor.Phys.87,1(1992)
- [27] A.S.Pikovsky,J.Kurths,Phys.Rev.Lett.72,1644(1994)
;A.S.Pikovsky,J.Kurths,Phys.D 76,411(1994)
- [28] K.Krischer,A.Mikhailov,Phys.Rev.Lett.73,3165(1994)
- [29] D.Battogtokh,M.Hildebrand,K.Krischer,A.Mikhailov,
Phys.Rep.288,435(1997)
- [30] N.B.Ouchi,K.Kaneko,Chaos 10, 359(2000)